Maintaining protein homeostasis: early and late endosomal dual recycling for the maintenance of intracellular pools of the plasma membrane protein Chs3

Irene Arcones, Carlos Sacristán†, and Cesar Roncero*
IBFG and Departamento de Microbiología y Genética, CSIC/Universidad de Salamanca, 37007 Salamanca, Spain

ABSTRACT The major chitin synthase activity in yeast cells, Chs3, has become a paradigm in the study of the intracellular traffic of transmembrane proteins due to its tightly regulated trafficking. This includes an efficient mechanism for the maintenance of an extensive reservoir of Chs3 at the *trans*-Golgi network/EE, which allows for the timely delivery of the protein to the plasma membrane. Here we show that this intracellular reservoir of Chs3 is maintained not only by its efficient AP-1–mediated recycling, but also by recycling through the retromer complex, which interacts with Chs3 at a defined region in its N-terminal cytosolic domain. Moreover, the N-terminal ubiquitination of Chs3 at the plasma membrane by Rsp5/Art4 distinctly labels the protein and regulates its retromer-mediated recycling by enabling Chs3 to be recognized by the ESCRT machinery and degraded in the vacuole. Therefore the combined action of two independent but redundant endocytic recycling mechanisms, together with distinct labels for vacuolar degradation, determines the final fate of the intracellular traffic of the Chs3 protein, allowing yeast cells to regulate morphogenesis, depending on environmental constraints.

INTRODUCTION

Yeast cells adapt to survive under many different situations, including highly stressful environmental conditions such as low nutrients, high temperature, high osmolarity, and diverse antifungal treatments. The plasma membrane undergoes continuous remodeling in response to these environmental changes by the transfer and removal of proteins and lipids via secretory and endocytic pathways. Endosomes are the places where the fate of internalized cell-surface proteins is decided (MacGurn *et al.*, 2012), and the major signal determining the destination of endocytosed plasma membrane (PM) proteins ("cargoes") is ubiquitin. Ubiquitin can act as a signal to promote

cargo endocytosis from the PM, but in many other cases, it only becomes critical later on the endocytic pathway. Ubiquitination of transmembrane proteins in yeast is mainly performed by Rsp5, a conserved ubiquitin ligase of the Nedd4 family (MacGurn *et al.*, 2012). Rsp5 is assisted by a series of adaptors that include the recently described arrestin-related trafficking adaptors (ARTs), which confer cargo specificity to those proteins lacking a PPxY motif with which Rsp5 can interact (Nikko and Pelham, 2009). Accordingly, Art proteins participate in the endocytosis and down-regulation of numerous plasma membrane transporters (Lin *et al.*, 2008; Nikko and Pelham, 2009; Becuwe *et al.*, 2012; Zhao *et al.*, 2013; Alvaro *et al.*, 2014; Crapeau *et al.*, 2014; O'Donnell *et al.*, 2015). Once at the endosomes, and depending on their ubiquitination state, cargoes can be transported to different destinations. On one hand, cargoes can be recognized by the endosomal sorting complex required for transport (ESCRT) and sorted into the lumen of the endosomes in a process known as multivesicular body (MVB) biogenesis, which results in degradation of the protein (Henne *et al.*, 2011), and on the other hand, cargoes can be recycled. In *Saccharomyces cerevisiae*, the endosomal recycling relies on at least two independent mechanisms. The first one depends on clathrin-coated vesicles (CCVs) and three different sets of adaptors: the AP-1 complex, GGAs, and the epsin-like proteins, which recruit clathrin to the membranes, facilitating the

---

loading of different cargoes (Robinson, 2015). The second mechanism is mediated by the retromer complex (Seaman, 2012), whose assembly is coordinated by Ypt7 and can be divided into two subcomplexes: a trimer of the Vps35, Vps29, and Vps26 proteins, which is mostly responsible for cargo selection, and a dimer of the Vps5 and Vps17 proteins, members of the sorting nexin (Snx) family believed to mediate tubule or vesicle formation (Seaman, 2012). The existence of specific adaptors for the recognition of some retromer cargoes, such as the iron complex transporter Ftr1-Fet3 (Strochlic et al., 2008), has also been described. However, the signals mediating cargo recognition remain largely elusive. The functional relationship between CCVs and the retromer complex in regard to recycling and whether recycled proteins follow a specific pathway are not fully understood. It is assumed that the differential distribution of proteins Vps21/Ypt5 and Ypt7 contribute to the establishment of early and late endosomal compartments and the two forms of recycling (Spang, 2009). Both forms coexist in all eukaryotic cells, acting on different sets of proteins and carrying out different biological functions (for recent reviews, see Seaman, 2012; Bonifacino, 2014). One notable exception to this is the yeast Golgi-resident protein Ste13, which seems to be actively maintained at the *trans*-Golgi network (TGN) by both AP-1–mediated (Foote and Nothwehr, 2006) and retromer-mediated (Nothwehr et al., 2000) recycling.

A critical step in yeast biology is the maintenance of cell integrity in variable and unpredictable environments, which is guaranteed by the continuous remodeling of the cell wall—the indispensable structure surrounding yeast cells (Levin, 2011). Chitin is an essential component of the yeast cell wall, acting as a scaffold for the assembly of the rest of its components (Cabib and Arroyo, 2013). In yeast, but also in other types of fungi, the protein Chs3 is the catalytic subunit of the major chitin synthase, chitin synthase III (CSIII; Roncero, 2002). The intracellular traffic of Chs3 to the PM is tightly controlled and allows the precise regulation of CSIII in order to preserve cell integrity (Levin, 2011).

Arrival of Chs3 at the PM from the Golgi depends on exomer (Sanchatjate and Schekman, 2006; Trautwein et al., 2006). However, Chs3 can still reach the PM in the absence of exomer by either deleting the AP-1 complex (Valdivia et al., 2002) or preventing their interaction through distinct mutations in the N-terminal cytosolic region of Chs3 (Starr et al., 2012). Moreover, Chs3 can also reach the PM when both exomer and epsins Ent3/5 are absent (Copic et al., 2007). Based on this, AP-1 and Ent3/5 have been proposed to participate in the endosomal recycling of Chs3 in order to maintain an intracellular reservoir of Chs3 at the TGN/early endosome (EE) boundary, from where Chs3 can be readily mobilized to the PM during the different phases of the cell cycle (Zanolari et al., 2011) or after cellular stress (Valdivia and Schekman, 2003). An early endosomal recycling has been described for other PM proteins, including the vesicle soluble *N*-ethylmaleimide–sensitive factor attachment protein receptor protein Snc1, whose recycling depends on Rcy1 (Chen et al., 2011) but also on the sorting nexins Snx4/41/42, which seem not to be involved in the traffic of Chs3 (Hettema et al., 2003). However, the trafficking model in which exomer and AP-1 functions somehow coordinate is restricted to a limited set of highly polarized proteins, including only Fus1 (Barfield et al., 2009) and Pin2 (Ritz et al., 2014). In contrast to Fus1 and Pin2, Chs3 is a polytopic protein sharing structural similarity with many transmembrane transporters and also shares with some of them the requirement for dedicated chaperones at the endoplasmic reticulum (ER; Kota and Ljungdahl, 2005). In general, the function of these transporters does not rely on endosomal recycling but on their regulated endocytosis and subsequent transport to the vacuole (Lauwers et al., 2010). However,

some yeast PM transporters have been shown to be dependent on the retromer function in order to be recycled, such as the iron or arginine transporters Ftr1 (Strochlic et al., 2008) and Can1 (Shi et al., 2011), respectively. Furthermore, a potential role for AP-1 in the recycling of the general amino acid permease Gap1 from the endosome under nitrogen starvation has been proposed (O'Donnell et al., 2010).
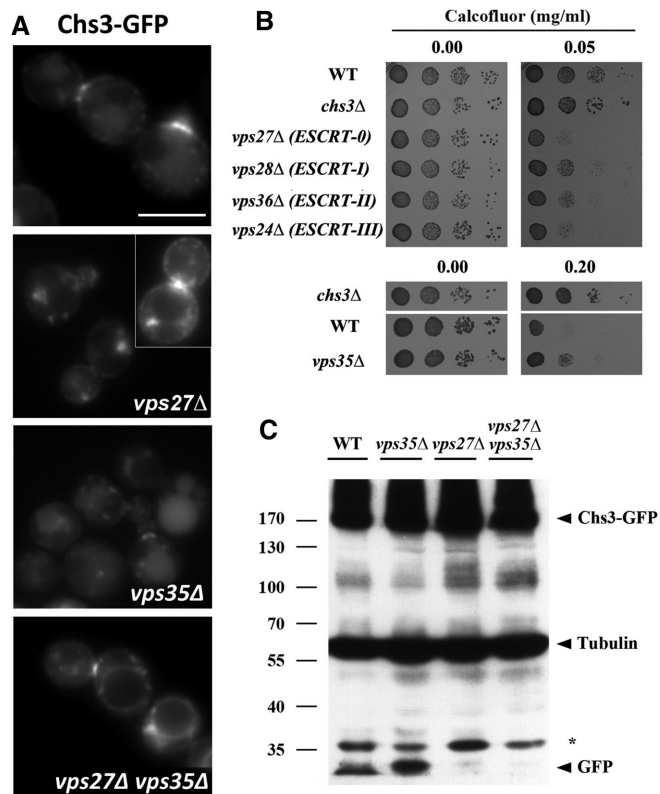
The current model for Chs3 intracellular trafficking has led to the proposal that Chs3 avoids vacuolar degradation (Ziman et al., 1996; Valdivia et al., 2002). The mechanism by which the bulk of Chs3 evades degradation, however, remains unclear. Here we demonstrate that Chs3 regularly transits through the late endosomal compartment and identify Chs3 as a new retromer cargo, thus characterizing a new recycling mechanism for Chs3 that contributes to the maintenance of the intracellular reservoir of Chs3 at the TGN/EE boundary. Moreover, we also identify Chs3 as a target of the Rsp5/Art4 ubiquitination complex at the PM, a system that would tag Chs3 for degradation at the vacuole, allowing yeast cells to discriminate between different intracellular populations of Chs3. These processes working together could contribute to regulation of CSIII, allowing yeast cells to remodel their cell wall based on environmental cues.

RESULTS

Chs3 transits the late endosomal compartment

Most Chs3 protein populates an intracellular reservoir at the TGN/EE compartment, from where it is delivered to the PM in a temporally and spatially controlled manner (Ziman et al., 1996; Valdivia et al., 2002; Zanolari et al., 2011). Based on these observations, it has been concluded that AP-1 effectively retains Chs3 in this reservoir, avoiding its degradation in the vacuole (Valdivia et al., 2002; Starr et al., 2012). In contrast to this, we consistently observed faint vacuolar staining of Chs3–green fluorescent protein (GFP; Figure 1A), whose intensity varied between strains and growth conditions. This observation suggested that a fraction of Chs3 was transported to the vacuole for degradation and the amount of this fraction might depend on growth conditions. We therefore hypothesized that the fate of Chs3 (degradation vs. recycling) could be regulated within endosomes.

To test this hypothesis, we disrupted MVB biogenesis based on the premise that if Chs3 was only being recycled to the TGN, its trafficking would be unaffected in ESCRT mutants. In the case that it was partially degraded, there would be a loss of staining in the degradative compartment. We found that in the *vps27Δ* mutant, defective in the ESCRT-0 complex and thus unable to internalize proteins into the MVB, Chs3 localized at the neck and intracellular spots similar to the wild-type strain. However, most cells (70.0 ± 6.3%) also showed a clear accumulation of Chs3 in the previously described class E compartment (Raymond et al., 1992), an enlarged vesicular structure caused by the collapse of endosomes (Piper et al., 1995). In addition, mutant cells showed reduced staining at the vacuolar compartment (Figure 1A and Supplemental Figure S1A). Similar results were obtained in other yeast strains carrying mutations in the ESCRT I, II, and III complexes (Supplemental Figure S1C). None of the ESCRT mutants showed calcofluor resistance, but a slightly higher sensitivity was noted compared with the control, which was probably due to the pleiotropic effects of the mutations (Figure 1B). Next we addressed Chs3-GFP localization in the retromer mutant *vps35Δ* (Seaman et al., 1997). In this case, Chs3-GFP localization in the vacuole was increased in a fraction of the cells (Figure 1A), consistent with an augmented degradation. In addition, the *vps35Δ* mutant was moderately resistant to calcofluor compared with the

A Chs3-GFP

vps27Δ

vps35Δ

vps27Δ vps35Δ

B

Calcofluor (mg/ml)

	0.00	0.05
WT		
chs3Δ		
vps27Δ (ESCRT-0)		
vps28Δ (ESCRT-I)		
vps36Δ (ESCRT-II)		
vps24Δ (ESCRT-III)		

	0.00	0.20
chs3Δ		
WT		
vps35Δ		

C

WT   vps35Δ   vps27Δ   vps27Δ vps35Δ

170 — ◄ Chs3-GFP
130 —
100 —
70 —
55 — ◄ Tubulin
40 —
35 — *
        ◄ GFP

FIGURE 1: Chs3 transits through the late endosomal compartment. (A) Localization of Chs3-GFP in the indicated ESCRT and retromer mutants. Note the clear appearance of the vacuolar space in the *vps27Δ* mutant and the appearance of neat signals in the vacuolar limiting membrane in the double *vps27Δ vps35Δ* mutant. In both strains, the retention of Chs3 in the class E compartment can be observed. (B) Calcofluor resistance of the indicated mutants. Note the hypersensitivity of all ESCRT mutants but the moderate resistance of the retromer (*vps35Δ*) mutant. (C) Western blot showing the amounts of Chs3-GFP and tubulin in the indicated mutants. Note the band corresponding to the vacuolar free form of GFP.

control, a phenotype compatible with lower functional levels of Chs3 (Figure 1B). The localization of Chs3-GFP in the double *vps27Δ vps35Δ* mutant proved to be much more conclusive (Figure 1A and Supplemental Figure S1A). Chs3-GFP was localized at the neck and intracellular spots corresponding to TGN and also at the class E compartment, as well as, remarkably, at the vacuolar limiting membrane in >80% of cells (Supplemental Figure S1A), suggesting a role for the retromer in retrieving Chs3 from late endosomes in case the protein was not internalized into intralumenal vesicles (ILVs). Similar results were obtained with a Chs3-2xGFP expressed from the endogenous locus (Supplemental Figure S1B). However, in all mutants, Chs3 still exhibited a reasonably normal distribution between the neck and the TGN reservoir, in agreement with normal levels of chitin assessed by calcofluor staining (unpublished results), which suggests that only a fraction of Chs3 is trafficked regularly through the late endosomal compartment. Of importance, the localization of Snc1, another integral membrane protein subjected to endocytic recycling through the early endosome, was not affected in any of these mutants (Supplemental Figure S1D).

To confirm these observations, we also addressed Chs3 levels by Western blot analysis. Quantifying the total amount of Chs3 is not an accurate measurement of its late endosomal trafficking due to

the major accumulation of Chs3 at the TGN. Therefore we focused on the presence of the free (vacuolar) form of GFP after the processing of Chs3-GFP in the vacuole (Figure 1C). This free GFP was observed in the wild-type strain, but its level increased significantly in the *vps35Δ* mutant, indicating a higher degradation level of Chs3-GFP. In contrast, free GFP was not observed in either the *vps27Δ* or *vps27Δ vps35Δ* mutant (Figure 1C), likely due to the failure in the formation of ILVs (Raymond *et al.*, 1992; Russell *et al.*, 2012).

Taken together, our results support not only the trafficking of Chs3-GFP through the late endosomal compartment and its degradation in the vacuole, but also the existence of a recycling mechanism from the late endosomal compartment mediated by the retromer complex.

Chs3 is recycled from late endosomes by the retromer complex, depending on its N-terminal domain

Recycling by the retromer complex would require an effective recognition of Chs3 as cargo. It has been shown that Chs3 interacts with other traffic complexes by its cytosolic N- and C-terminal domains. For example, discrete N-terminal regions of Chs3 are involved in its interaction with the AP-1 complex in the early endosomes (Starr *et al.*, 2012). In addition, this region has also been proposed to mediate effective exomer recognition (Starr *et al.*, 2012; Weiskoff and Fromme, 2014), whereas the C-terminal domain is fully required for its interaction with the exomer (Rockenbauch *et al.*, 2012). On the basis of this evidence, we tested the localization of the N-terminal ($^{\Delta126}$Chs3) and C-terminal (Chs3$^{\Delta37}$) truncated forms of Chs3 in the *vps27Δ* and *vps35Δ* mutants. Neither of these truncated Chs3 proteins showed differential localization in the *vps35Δ* mutant compared with the wild-type strain (Supplemental Figure S2A), but their localization was affected in the *vps27Δ* ESCRT mutant (Figure 2A). Chs3, $^{\Delta126}$Chs3, and Chs3$^{\Delta37}$ accumulated at the class E compartment in the *vps27Δ* mutant, but only $^{\Delta126}$Chs3 localized extensively at the vacuolar membrane (Figure 2A), similar to wild-type Chs3 in the double *vps27Δ vps35Δ* mutant. We therefore concluded that the N-terminal, but not the C-terminal, part of Chs3 was required for retromer retrieval. Next we addressed the importance of different regions in this N-terminal cytosolic domain. Proteins lacking only the first 63 amino acids did not accumulate at the vacuolar membrane. However, deletion of the region between amino acids 63 and 125, as well as other more extensive deletions, induced the accumulation of these proteins at this location in >85% of the cells in the *vps27Δ* mutant (Figure 2A). Moreover, the $^{\Delta126}$Chs3 and $^{\Delta63-125}$Chs3 proteins also led to higher levels of free GFP than the full-length protein (Figure 2B). Both lines of evidence indicated that the absence of the N-terminal region of Chs3 recapitulates the effects caused by the *vps35Δ* mutation, highlighting the importance of this region in the retromer-mediated retrieval.

To confirm these results biochemically, we addressed the physical Vps35/Chs3 interaction at the late endosomal compartment by coimmunoprecipitation (coIP) experiments. Coimmunoprecipitation between both proteins was not detected in the wild-type strain even after dithiobis(succinimidylpropionate) (DSP) cross-linking but was revealed after blocking late endosomal transit through the ESCRT-I mutant *vps28Δ* (Figure 2C and Supplemental Figure S2B; Shi *et al.*, 2011), indicating physical interaction between both proteins in the late endosomal compartment. Moreover, the level of coIP of Vps35 with $^{\Delta63-125}$Chs3 protein was reduced to about one-fourth, pointing toward reduced interaction between the proteins and explaining the accumulation of $^{\Delta63-125}$Chs3 at the vacuolar membrane. Of interest, $^{\Delta63-125}$Chs3 protein oligomerization was normal, and the protein was fully exported from the ER after *CHS7* overexpression. However, it
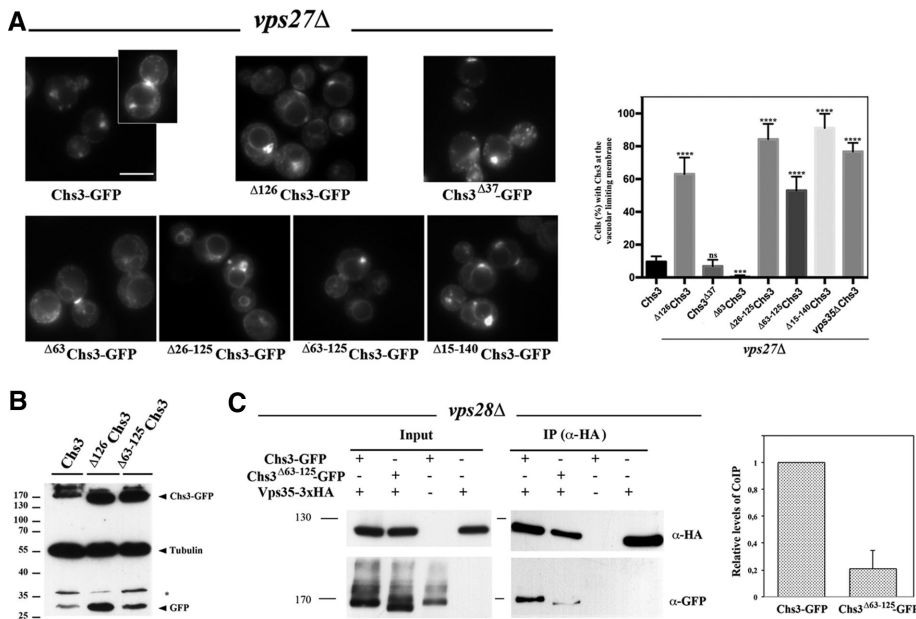
FIGURE 2: The role of the N- and C-terminal regions of Chs3 in its trafficking through the LE pathway. (A) Localization of the indicated forms of Chs3-GFP in the *vps27Δ* mutant. In this strain, the different forms of Chs3 accumulate in the class E compartment and the vacuolar space is clear in all cases, but only some of the constructs stain the vacuolar limiting membrane. The graph represents the percentage of cells showing vacuolar membrane staining for each construct, including the numerical value for Chs3 in the double mutant *vps27Δ vps35Δ*. Note the absence of this signal for wild-type, $^{\Delta63}$Chs3, and Chs3$^{\Delta37}$ proteins. (B) Western blot showing the amounts of Chs3-GFP and tubulin for the indicated constructs. Note that the band corresponding to the vacuolar free form of GFP increased for proteins lacking the N-terminal domain. (C) CoIP assay after DSP cross-linking, showing Vps35/Chs3 interaction in the ESCRT mutant *vps28Δ*. Vps35 was immunoprecipitated with the anti-HA antibody, and the precipitate was developed with the anti-HA or anti-GFP as indicated. Note the significant levels of coIP between Chs3 and Vps35 proteins but the reduced coIP levels between Vps35 and $^{\Delta63-126}$Chs3. Quantitative analysis of the CoIP is presented in the graph representing the relative amounts of coimmunoprecipitated protein compared with the immunoprecipitated bait. The data included represent the average of four independent experiments.

still confers a calcofluor resistance phenotype (Supplemental Figure S2, C–E; Sacristan *et al.*, 2013), which is similar to that observed in the *vps35Δ* mutant (Figure 1B), a result compatible with its presumably poor recycling from the late endosomal compartment.
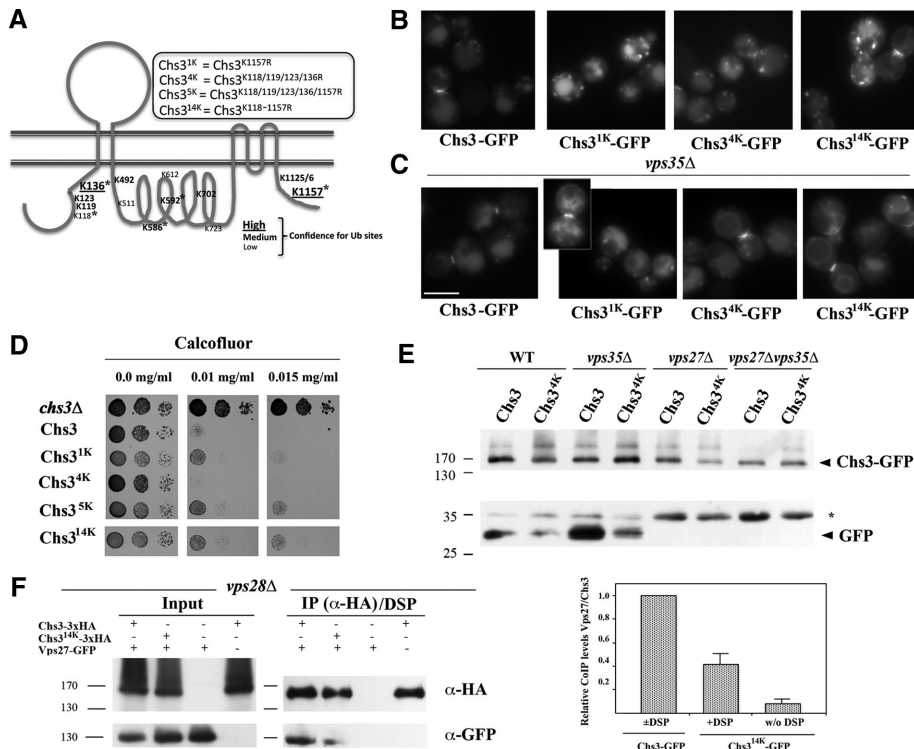
Late endosomal trafficking of Chs3 is linked to its ubiquitination status

The transit of proteins through the late endosome (LE) is usually associated with vacuolar degradation. This process is linked to the ESCRT complex, which has been implicated in the recognition of ubiquitinated proteins for their later internalization through the formation of ILVs, a required step for protein degradation at the vacuole (Raiborg and Stenmark, 2009). Therefore it would be expected that Chs3 traffic through the late endosome depends on its ubiquitination. Chs3 contains 14 potential ubiquitin sites, based on bioinformatics analysis (Figure 3A), several of which have been shown experimentally to be ubiquitinated (Swaney *et al.*, 2013). N- and C-terminal regions of Chs3 have been shown to be important for traffic of Chs3 (see earlier discussion; Weiskoff and Fromme, 2014). Hence, we initiated our work by replacing the nearby N-terminal lysines 118, 119, 123, and 136 with arginine residues to create the Chs3^{4K} protein (Figure 3A). In addition, we separately replaced the C-terminal K1157 in Chs3^{1K} and all 14 of the lysine residues predicted to be ubiquitinated in the Chs3^{14K}

constructs (see *Materials and Methods* for details on these constructions). The traffic of these proteins was assessed in different mutant strains by fluorescence microscopy. In the wild-type strain, all mutated proteins were localized at the neck and in intracellular spots (Figure 3B), similar to the wild-type Chs3 protein. No altered intracellular localizations were observed in the *vps27Δ* mutant. However, inhibiting the retromer function by deleting *VPS35* localized Chs3^{4K}-GFP and Chs3^{14K}-GFP proteins at the vacuolar membrane in most cells (>70%), similar to the wild-type protein in the *vps27Δ vps35Δ* double mutant (Figure 3C). This result suggested that these modified proteins might not be recognized by the ESCRT complex and, as result, not be incorporated into ILVs. Moreover, the Chs3^{4K}-GFP protein conferred slight hypersensitivity to calcofluor, whereas the other truncations, all of which contain the K1157R mutation, were moderately calcofluor resistant compared with the wild type (Figure 3D). Taken together, our results not only showed the biological relevance of Chs3 ubiquitination, but also suggested differential roles for the N- or C-terminal ubiquitination, in agreement with the different biological roles proposed for these domains. Of interest, the protein lacking the 14 lysine residues, Chs3^{14K}-GFP, recapitulated the phenotypes associated with the absence of ubiquitin in both domains.

The foregoing results directly link N-terminal ubiquitination of Chs3 with its transit through the late endosomal compartment and thus with its recognition by the ESCRT machinery, suggesting that this protein avoids degradation at this compartment. This in fact turns out to be the case, since Chs3^{4K}-GFP produced reduced levels of free GFP in both wild-type and *vps35Δ* strains compared with the wild-type Chs3-GFP (Figure 3E). Moreover, in agreement with the microscopic data, Chs3^{14K}-GFP also led to reduced levels of free GFP in all strains tested (Supplemental Figure S3B). However, in both cases, degradation was not completely abolished as in the *vps27Δ* mutant (Figure 3E and Supplemental Figure S3B), in agreement with the partial lumenal staining of the vacuole produced by Chs3^{4K}-GFP and Chs3^{14K}-GFP proteins (Figure 3C; see also Supplemental Figure S3C). On the basis of these results, we then addressed the physical interaction between Chs3 and ESCRT complex by coIP experiments. Vps27 coimmunoprecipitated with Chs3 in the *vps28Δ* mutant, using protein extract treated or not with the cross-linking agent DSP (Supplemental Figure S3D), a clear indication of the physical interaction between the proteins. Moreover, coIP was significantly reduced when the Chs3^{14K} was used (Figure 3F and Supplemental Figure S3D), highlighting the importance of Chs3 ubiquitination in ESCRT recognition.

In conclusion, the late endosomal traffic of Chs3 depends on its ubiquitination at defined lysine residues within its N-terminal cytosolic domain. This ubiquitination is recognized by the ESCRT machinery to trigger Chs3 degradation at the vacuole.

A

Chs3^{1K} = Chs3^{K1157R}
Chs3^{4K} = Chs3$^{K118/119/123/136R}$
Chs3^{5K} = Chs3$^{K118/119/123/136/1157R}$
Chs3^{14K} = Chs3$^{K118-1157R}$

K136* K492 K612
K123 K511 K1125/6
K119 K592* K702 K1157*
K118* K586* K725

High
Medium } Confidence for Ub sites
Low

B

Chs3-GFP   Chs3^{1K}-GFP   Chs3^{4K}-GFP   Chs3^{14K}-GFP

C

vps35Δ

Chs3-GFP   Chs3^{1K}-GFP   Chs3^{4K}-GFP   Chs3^{14K}-GFP

D

Calcofluor

	0.0 mg/ml	0.01 mg/ml	0.015 mg/ml
chs3Δ			
Chs3			
Chs3^{1K}			
Chs3^{4K}			
Chs3^{5K}			
Chs3^{14K}			

E

WT   vps35Δ   vps27Δ   vps27Δvps35Δ

Chs3 Chs3^{4K} Chs3 Chs3^{4K} Chs3 Chs3^{4K} Chs3 Chs3^{4K}

170 —
130 —   ◄ Chs3-GFP

35 —   *
25 —   ◄ GFP

F

vps28Δ

Input   IP (α-HA)/DSP

Chs3-3xHA   + - - +   + - - +
Chs3^{14K}-3xHA - + - -   - + - -
Vps27-GFP   + + + -   + + + -

170 —
130 —   α-HA

130 —   α-GFP

Relative CoIP levels Vps27/Chs3
1.0
0.8
0.6
0.4
0.2
±DSP   +DSP   w/o DSP
Chs3-GFP   Chs3^{14K}-GFP

FIGURE 3: Ubiquitination regulates Chs3 traffic. (A) Bioinformatic prediction of Chs3 ubiquitination sites (UbPred; www.ubpred.org). The asterisk marks the lysine sites confirmed experimentally to be ubiquitinated (Swaney et al., 2013). Replacement of the indicated lysine residues by arginines was carried out to create the different Chs3 mutants indicated. (B) Localization of the different Chs3 constructs in the wild-type strain. Note the similarity of the staining. (C) Localization of the different forms of Chs3-GFP in the vps35Δ mutant. Note the neat staining at the vacuolar limiting membrane in only the Chs3^{4K}- and Chs3^{14K}-containing strains. (D) Resistance to calcofluor of the strains carrying the different forms of Chs3 as a single copy in the pRS315 plasmid. (E) Western blot of the total extract from the indicated strains containing Chs3-GFP or Chs3^{4K}-GFP. Both are from the same Western blot, but the lower blot is overexposed to highlight the free GFP band. Note the reduced liberation of free GFP from Chs3^{4K} constructs. (F) CoIP between Chs3/Chs3^{14K} and Vps27. Protein extracts were obtained from cells of the vps28Δ mutant (Shi et al., 2011) containing the indicated construct. Experiments were performed after DSP cross-linking. Chs3-3xHA was immunoprecipitated with the anti-HA antibody and the immunoprecipitated developed with anti-HA or anti-GFP as indicated. Relative levels of CoIP are shown in the graph, and the values are the average of two independent experiments. Note the reduced level of CoIP between the Chs3^{14K} and Vps27 proteins, which is indicative of the poor recognition of the nonubiquitinated Chs3 protein by the ESCRT complex.

## Chs3 is ubiquitinated at the PM, depending on the Rsp5 ubiquitin ligase

Our results highlight the functional relevance of Chs3 ubiquitination, but the overall levels of such ubiquitination, as well as the molecular machinery involved in the process, remain unknown. We consequently addressed the ubiquitination status of Chs3 by different methods. Western blot results of the ubiquitinated forms of Chs3 were not reliable. Therefore we used a technique based on the inducible expression of ubiquitin tagged with the heptahistidine (7xHis) epitope followed by purification of total ubiquitinated proteins using Co^{2+}-TALON resin and further Western blot analysis for detection of Chs3–triple hemagglutinin (3xHA; Parker et al., 2007). The purification of ubiquitinated proteins reproducibly yielded three bands of ~149, 176, and 240 kDa that were not present in the controls lacking tagged ubiquitin (Figure 4A). The most abundant band was that of 149 kDa, which was barely visible in the pull downs of control cells (Figure 4A) and showed a slightly lower mobility than

the nonubiquitinated form of Chs3. The Chs3^{4K}-GFP protein did not show discernible differences in its ubiquitination pattern, but the protein lacking all predicted ubiquitination sites, Chs3^{14K}-GFP, clearly showed an altered and overall reduced pattern of ubiquitination (Figure 4A), confirming the ubiquitinated status of Chs3.

Considering the intracellular localizations reported for Chs3, the Rsp5 ubiquitin-ligase was the most likely candidate for Chs3 ubiquitination. We therefore addressed the behavior of Chs3 in the temperature-sensitive rsp5-1^{ts} mutant. Even at the permissive temperature, the rsp5-1^{ts} cells were extremely sensitive to calcofluor and showed an altered localization for Chs3-GFP, but, more important, upon incubation at restrictive temperature, Chs3 was poorly ubiquitinated in the rsp5-1^{ts} mutant, producing a diffuse pattern of bands (Figure 4B) similar to the one described for the Chs3^{14K}-GFP protein. These results suggest that Chs3 is ubiquitinated by Rsp5 at multiple sites, but they do not indicate where the ubiquitination of Chs3 occurred, since Rsp5 has been described to act at multiple intracellular compartments. Chs3 acts at the PM, and therefore we checked whether Chs3 ubiquitination occurred here by testing the status of Chs3 ubiquitination in different mutants that showed higher levels of Chs3 at the PM because of the reduced levels of Chs3 endocytosis (Reyes et al., 2007; Sacristan et al., 2012). As predicted, the level of ubiquitinated Chs3 increased in the syp1Δ and rvs161Δ mutants but also after blockage of endocytosis by latrunculin A (LatA; Figure 4C). Of interest, the amount of the 149-kDa band did not change significantly compared with the control, but in all cases, the intensity of the 176- and 240-kDa bands (double and triple asterisks) increased significantly. Thermal stress also blocks endocytosis in a transitory way (Lilie and

Brown, 1994; Delley and Hall, 1999) and increases Chs3 accumulation at the PM (Valdivia and Schekman, 2003). Accordingly, we observed that the overall ubiquitination levels of Chs3 increased significantly after a temperature upshift (Figure 4C). Therefore all conditions that triggered Chs3 accumulation at the PM resulted in higher levels of Chs3 ubiquitination.

The general rules for the intracellular traffic of Chs3 were established some time ago, with the existence of several mutants that block Chs3 traffic at different steps (Roncero, 2002). Specifically, the chs5Δ mutant blocks traffic of Chs3 at the TGN, avoiding its arrival at the PM (Santos and Snyder, 1997). Thus we determined Chs3 ubiquitination in this mutant and observed an overall reduction in the levels of Chs3 ubiquitination and the almost complete disappearance of the 176- and 240-kDa ubiquitinated bands. The 149-kDa band remained unaltered (Figure 4D). Moreover, Chs3 protein accumulated at high levels in the vacuolar membrane in the chs5Δ vps35Δ double mutant (Figure 4E), which is in agreement with its reduced
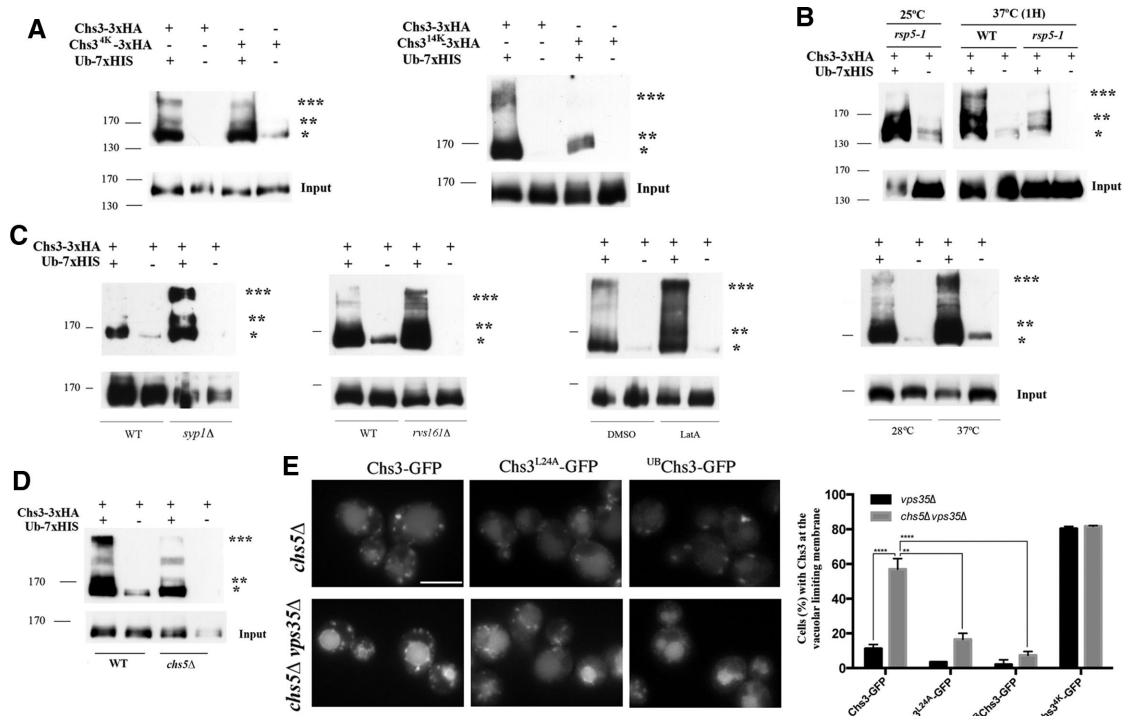
FIGURE 4: The ubiquitination status of Chs3. (A) Ubiquitination patterns of the indicated forms of Chs3. (B) Ubiquitinated forms of Chs3 in the *rps5-1* mutant grown at permissive and restrictive temperatures. Note the increased ubiquitination of Chs3 at 37°C in the wild type but also the reduced ubiquitinated forms of Chs3 in the *rps5-1* mutant at this temperature. (C) Ubiquitination of Chs3 in some endocytosis mutants, after LatA treatment and after thermal stress. Note the general increase of ubiquitination in all cases and also the distinct increased intensity of some bands. (D) Ubiquitination of Chs3 in the *chs5Δ* mutant. Note the significant reduction of bands indicated by double and triple asterisks. (E) Localization of the indicated forms of Chs3 in the *chs5Δ* or *chs5Δ vps35Δ* mutant. Note the significant accumulation of Chs3-GFP at the vacuolar limiting membrane, alleviated by the rerouting of the protein to the PM by the L24A mutation (Starr *et al.*, 2012). A permanent ubiquitin tag in the N-terminal of Chs3 (UBChs3-GFP) also prevents its accumulation in the vacuolar limiting membrane. The graph on the right represents the quantitative average data from three independent experiments. The statistical significance of the differences is indicated. To determine Chs3 ubiquitination patterns, total ubiquitinated proteins were first enriched using the Co^{2+}-TALON resin and separated in polyacrylamide gels, and blots were developed with the anti-HA antibody to visualize the tagged Chs3 protein. Note the occasional appearance of faint bands in the negative controls, most probably due to the nonspecific binding of Chs3-3xHA to the Co2+-TALON resin. Asterisks indicate the major forms of ubiquitinated Chs3 protein. Input images represent the relative levels of Chs3 protein in total cellular extracts, corresponding to one-fifth of the amount of protein enriched. See *Materials and Methods* and the text for more detailed explanations.

ubiquitinated state. Of interest, the Chs3^{L24A}-GFP protein, which bypasses the *chs5Δ* blockade at the TGN by reaching the PM through the alternative route (Starr *et al.*, 2012), and the UBChs3-GFP protein, with a permanent ubiquitin tag in the N-terminus, showed highly reduced vacuolar membrane accumulation in the *chs5Δ vps35Δ* mutant (Figure 4E). Thus blocking traffic of Chs3 at the TGN and preventing its transit through the PM reduced ubiquitination of Chs3 and prevented its recognition by the ESCRT complex. Taken together, our results indicate that Chs3 is ubiquitinated by Rsp5 at specific lysine residues at the PM and that this ubiquitination specifically targets Chs3 for degradation. However, they also suggest that not all Chs3 ubiquitination occurs at the PM, and therefore Chs3 could also be ubiquitinated at other residues at various intracellular localizations.

Chs3 ubiquitination at the PM depends on Art4/Rod1 α-arrestin

Protein ubiquitination by Rsp5 is frequently directed to specific substrates through the use of dedicated adaptor proteins. Among them, we focused on the α-arrestin family of proteins, most of which

have been linked to the ubiquitination of PM proteins (Nikko and Pelham, 2009). We screened *artΔ* mutants for calcofluor hypersensitivity or resistance (Figure 5A). The *art9/rim8Δ* mutant was resistant to calcofluor, as described in Gomez *et al.* (2009). By contrast, *art1Δ*, *art4Δ*, and *art6Δ* were highly sensitive to calcofluor. Next we determined the localization of Chs3 in all *artΔ* mutants in the *vps35Δ* background (Figure 5B and Supplemental Figure S4). Most arrestin mutants did not affect Chs3 localization, but the *art4Δ* mutant accumulated Chs3 at the vacuolar limiting membrane in ~50% of the cells (Figure 5, B and C), a value close to the one observed for the Chs3^{4K} used as a control. This phenotype was not observed in any of the other *artΔ* mutants (Supplemental Figure S4, A and B). Moreover, generation of free GFP at the vacuole from wild-type Chs3-GFP was significantly reduced in the *art4Δ vps35Δ* mutant compared with the single *vps35Δ* mutant, this reduction being equivalent to the one observed for Chs3^{4K}-GFP (Figure 5D). These results, taken together, link Art4/Rod1 function to late endosomal traffic of Chs3. Thus Art4/Rod1 might be the arrestin involved in Chs3 N-terminal ubiquitination after its transit through the PM.
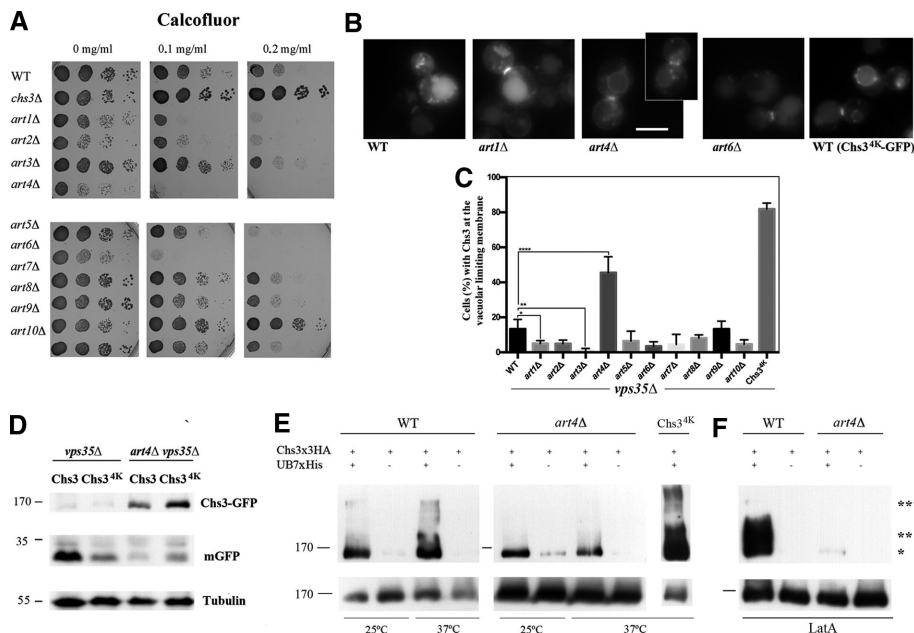
FIGURE 5: The role of Art4 in Chs3 trafficking. (A) Calcofluor resistance of the different arrestin (*art*Δ) mutants. Note the existence of hypersensitive and resistant mutants. (B) Localization of Chs3-GFP in the *vps35*Δ strain combined with different *art*Δ mutations as indicated and (C) quantitative analysis of the images; also see Supplemental Figure S4 for additional images. Note that only the *art4*Δ mutant shows significant accumulation of Chs3-GFP at the vacuolar limiting membrane. (D) Western blot showing Chs3-GFP levels in the *art4*Δ *vps35*Δ double mutant and the reduced liberation of free GFP. (E) Ubiquitination patterns of Chs3 in the *art4*Δ mutant after thermal stress at 37°C for 1 h. Note the lower amounts of ubiquitination in the *art4*Δ. Chs3^{4K} did not show apparent changes in the ubiquitination pattern compared with the control. (F) Ubiquitination patterns of Chs3 in the *art4*Δ mutant after LatA treatment for 1 h. Note the reduction of ubiquitination.

We wanted to test the hypothesis that Art4/Rod1 is the arrestin directly involved in the ubiquitination of Chs3. One outcome might be that the absence of Art4/Rod1 affected the Chs3 ubiquitination pattern. At 25°C, the *art4*Δ mutant showed an almost normal pattern of Chs3 ubiquitination but lacked the band corresponding to 176 kDa. This band was produced upon the arrival of Chs3 at the PM (Figure 4D), and increased significantly after Chs3 accumulation at the PM (Figure 4C). After a temperature shift to 37°C, the 176-kDa band became very intense in the wild type (Figure 5E) but was absent in the *art4*Δ mutant, indicating that Art4/Rod1 activity was indeed responsible for the ubiquitination of Chs3 and linked to this band. Surprisingly, Chs3^{4K}-GFP, which phenotypically resembled the *art4*Δ mutant (compare Figures 3C and 5B and the corresponding Supplemental Figures S3, A and C, and S4A), showed a normal pattern of ubiquitination, with a significant increase in the 176-kDa band at high temperature. Moreover, the absence of Art4 also very significantly reduced the level of Chs3 ubiquitination after the endocytosis blockade by LatA (Figure 5F). These results unequivocally link Art4/Rod1 to the ubiquitination of Chs3 on its transit through the PM but also point to additional sources of Chs3 ubiquitination.

Late endosomal recycling contributes to Chs3 homeostasis at the TGN after stress

The proper traffic of Chs3 in yeast cells relies on the maintenance of an extensive reservoir of the protein at the TGN/EE (Ziman *et al.*, 1996; Valdivia *et al.*, 2002). It is interesting that this intracellular reservoir is mostly depleted after some forms of cellular stress (Valdivia and Schekman, 2003) as a consequence of the accumulation of Chs3 at the PM that takes place in order to trigger increased levels

of chitin (Levin, 2011). To understand how yeast cells regain their intracellular reservoir of Chs3, we addressed Chs3 localization after cell stress in the *vps35*Δ mutant.

Thermal stress induced transient accumulation of Chs3 at the PM (Figure 6A; note the distribution of Chs3 along the PM; Valdivia and Schekman, 2003), a situation that was reverted after yeast adaptation at high temperature. Moreover, we showed that this temperature upshift not only increased Chs3 ubiquitination (Figure 4, B and C), but it also promoted a significant but transient accumulation of Chs3-GFP at the vacuolar limiting membrane in the *vps35*Δ mutant (Figure 6, A and B). The accumulation reached its maximum at 30 min (35% of the cells) and diminished afterward to reach control levels after 60 min of heat exposure (Figure 6B). LatA treatment also triggered Chs3 accumulation at the PM and the depletion of the TGN reservoir (Figure 6A; Reyes *et al.*, 2007). This phenotype can be reverted by washing out LatA. Of interest, after 20 min of the LatA washout, a peak of Chs3 accumulation at the vacuolar limiting membrane was also observed (Figure 6C). This accumulation was reduced after a longer incubation in the absence of the drug. The results coincide and suggest the existence of a pool of Chs3 that escaped ESCRT recognition and hence is neither incorporated in ILVs nor degraded. This protein would be susceptible to being recycled by the retromer, contributing to the regeneration of the TGN/EE pool of Chs3. Under the same conditions, accumulation of Chs3^{4K}-GFP at the vacuolar membrane was not significantly affected (Figure 6, B and C) due to its intrinsic inability to be recognized by the ESCRT complex. It is unclear whether this failure in degradation is linked to an inefficient ubiquitination of Chs3 after its massive accumulation at the PM or simply reflects the saturation of the degradative route. Independent of the final reason, this interpretation will situate the late recycling of Chs3 by the retromer as a complementary mechanism to regain internal pools of the protein after cellular stress.

DISCUSSION

Late endosomal traffic of Chs3: a new recycling pathway for CSIII

A very efficient mechanism for the endosomal recycling of Chs3 allows for the maintenance of an extensive intracellular reservoir of this protein at the TGN/EE boundary (Ziman *et al.*, 1996; Valdivia *et al.*, 2002). However, our results indicate that despite this extremely efficient recycling mechanism, mediated mainly by the AP-1 complex, Chs3 also traffics regularly through the late endosomal compartment.

What are the reasons for this traffic? Certainly, part of the Chs3 reaching the LE compartment is tagged for degradation at the vacuole, accounting for the clearance of potentially damaged proteins (MacGurn *et al.*, 2012). Nevertheless, the recycling of Chs3 by the retromer also indicates that late recycling contributes to replenishing the intracellular reservoir of Chs3 at the TGN. The precise amounts of Chs3 recycled along endosomal pathways are technically difficult
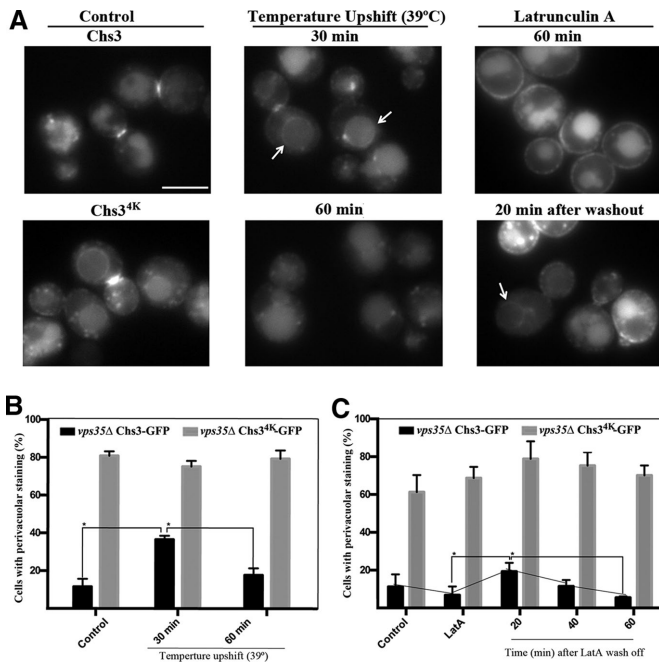
FIGURE 6: Chs3-GFP turnover after cell stress. (A) Microscopic localization of Chs3-GFP after temperature upshift or LatA treatment in the *vps35Δ* strain. Chs3[4K] is included as a control. (B) Quantitative analysis of cells showing staining at the vacuolar limiting membrane after the indicated times. Cells were grown at 25°C (control) and shifted to 39°C for 30 or 60 min. (C) Quantitative vacuolar limiting membrane localization after LatA treatment for 60 min and further recovery in the absence of the drug for the indicated times. In both cases, the graph represents the average of three independent experiments, and in all cases, the localization of Chs3[4K] was used as reference. Statistical analysis of the data (*$p < 0.05$).

to assess due to the complexity of Chs3 trafficking, but the moderate resistance of *vps35Δ* mutant to calcofluor suggests that retromer recycling, although probably minor, is not functionally negligible. The calcofluor resistance showed by cells containing [Δ63-125]Chs3, which is not efficiently recycled by the retromer, is also in line with the same idea. Thus our results showed that the intracellular reservoir of Chs3 at the TGN/EE is the consequence of not one but two independent recycling mechanisms—one mediated by the AP-1 complex (Valdivia *et al.*, 2002; Starr *et al.*, 2012) and the other mediated by retromer—the latter acting as a sort of additional mechanism for retrieving the Chs3 leakage to the LE compartment (Figure 7A). These results are consistent with those described for the Ste13 protein, although this protein contains a single transmembrane (TM) domain and does not reach the PM (Nothwehr *et al.*, 2000; Foote and Nothwehr, 2006). Of interest, both Chs3 (this work) and Ste13 (Nothwehr *et al.*, 2000; Foote and Nothwehr, 2006) rely on different N-terminal sequences for their interaction with AP-1 and retromer complexes, in clear agreement with the highly different mechanistic workflow described for these complexes (Seaman, 2012; Bonifacino, 2014).

The complementary action of these two mechanisms in the recycling of PM proteins with multiple TM domains has not been experimentally addressed, but it would be compatible with our knowledge on the intracellular traffic of Gap1 (Rubio-Texeira and Kaiser, 2006; O'Donnell *et al.*, 2010), raising the possibility that complementary action of AP-1 and retromer recycling mechanisms could be a much more general system for the recycling of TM proteins than previously believed.

A biological role for the Chs3 late endosomal traffic

Our results indicate that despite Chs3 being extensively ubiquitinated upon its transit through the PM, the nonubiquitinated Chs3 (Chs3[14K]) seemed to be endocytosed normally, suggesting that ubiquitination is not essential for Chs3 endocytosis. However, we cannot exclude the presence of additional ubiquitinated sites on Chs3 required for its endocytosis; alternatively, it is also possible that AP-2 could directly recognize specific regions of Chs3, promoting its endocytosis, as described in yeast for the Mid2 protein (Chapa-y-Lazo *et al.*, 2014). What becomes clear through this work is that the N-terminal ubiquitination of Chs3 regulates its intracellular traffic. This ubiquitination signal does not seem to affect Chs3 recognition by either the retromer or AP-1 complexes since the Chs3[4K] protein, lacking N-terminal ubiquitination, did not accumulate at the vacuolar membrane or reach the PM in the *chs5Δ* mutant. However, N-terminal ubiquitination allows efficient Chs3 recognition by the ESCRT complex, its incorporation into ILVs, and its further degradation at the vacuole, which in turn impedes its retromer-mediated recycling. Ubiquitination signaling for PM proteins has been described as a way to degrade undesired proteins for different reasons, including changes in cellular metabolism (Becuwe *et al.*, 2012; Becuwe and Léon 2014) or improperly folded conformations (Zhao *et al.*, 2013). We do not know the precise reasons for differentiating the Chs3 reaching the PM, but they seem biologically relevant since the cells actively discriminate the protein unable to reach the PM, as in the *chs5Δ* mutant, by preventing its N-terminal ubiquitination and its degradation in the vacuole. Moreover, the introduction of an exogenous ubiquitin tag in the N-terminal region of Chs3 allows its recognition by the ESCRT machinery and its concomitant vacuolar degradation even in the absence of traffic through the PM.

An alternative but not excluding explanation could be that this late endosomal recycling also contributes to maintaining stable intracellular pools of Chs3. This possibility is in agreement with our results showing that cells do not fully process for degradation all of the Chs3 accumulated at the PM after thermal stress or release from endocytosis blockade (Figure 6). The depletion of the intracellular pools of Chs3 after cellular stress followed by its ubiquitin-mediated complete degradation would compromise cell integrity upon growth restoration. Therefore regulation of Chs3 degradation combined with late endosomal recycling seems to be a way to contribute effectively to the maintenance of Chs3 intracellular levels (Figure 7B).

The decision: how to orchestrate the endosomal traffic of Chs3

We showed that α-arrestin Art4/Rod1 assisted ubiquitin ligase Rsp5 in Chs3 ubiquitination, probably because of the inefficient recognition of Chs3 by the ubiquitin ligase Rsp5 (Belgareh-Touzé *et al.*, 2008). Our results clearly indicate that this Art4-dependent ubiquitination is linked to the transit of Chs3 through the PM, although we cannot confirm whether this ubiquitination occurs precisely at the PM. Moreover, the similarity of the phenotypes found for *art4Δ* and Chs3[4K] mutants strongly suggested that Art4/Rod1 is directly involved in the N-terminal ubiquitination of Chs3, thus being a major player in the orchestration of the late endosomal traffic of Chs3. However, the ubiquitination pattern observed for Chs3 in the *art4Δ* mutant is different from that of Chs3[4K] (Figure 5E), suggesting that Art4/Rod1 mediates Chs3 ubiquitination beyond its N-terminal region. The potential function for this additional ubiquitination remains unexplored.

The results reported here are fully consistent with the biological function proposed for arrestins (Lin *et al.*, 2008; Becuwe and Léon 2014; Crapeau *et al.*, 2014; O'Donnell *et al.*, 2015). However, Chs3
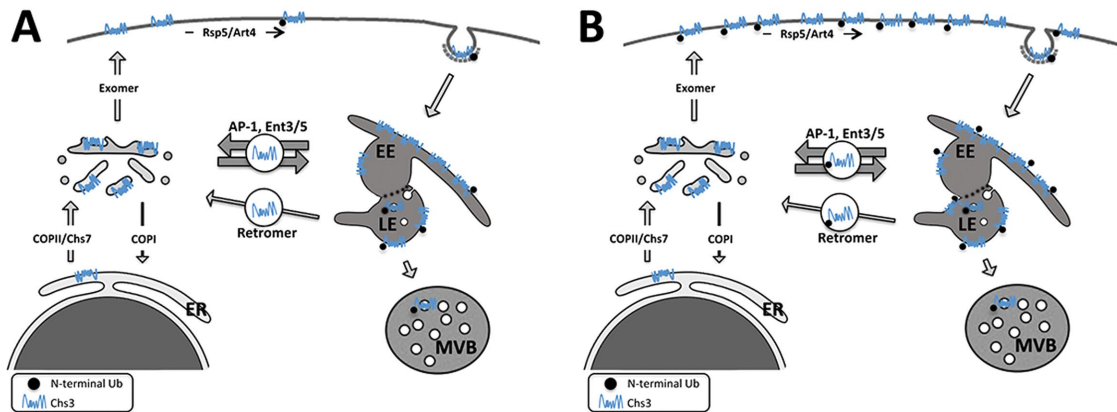
FIGURE 7: Adaptation of the endosomal recycling of Chs3 to physiological conditions. (A) Under normal growth conditions, most Chs3 accumulates at the TGN/EE boundary, an intracellular reservoir replenished by the continuous supply of Chs3 from the ER. This reservoir is maintained by an extremely efficient endosomal recycling of Chs3 by the AP-1/Ent3/5 functions, preventing Chs3 degradation in the vacuole. The small amount of Chs3 that reaches the LE can be recycled back to TGN by the retromer, which acts as a safeguard mechanism. From this intracellular reservoir, a part of Chs3 is delivered by the exomer to the PM, where it is ubiquitinated at its N-terminal region by the Rsp5/Art4. This ubiquitin-tagged protein is endocytosed and travels to the LE compartment, where it is incorporated into ILVs for degradation in the vacuole. Accordingly, yeast cells distinguish the Chs3 protein that has been transported through the membrane from that retained at the TGN/EE. (B) Cellular stress triggers massive accumulation of Chs3 at the PM, depleting the TGN/EE reservoir. Under these conditions Chs3 is mostly ubiquitinated. On growth restoration, Chs3 is endocytosed, saturating the AP-1/Ent3/5 recycling mechanism and reaching the LE. Subsequently Chs3 is recycled by the retromer, which in this case contributes significantly to replenishing the TGN reservoir, avoiding massive Chs3 degradation. The color intensity and the width of the arrows reflect the relative contribution of these pathways to Chs3 trafficking. The model describes only the role of N-terminal ubiquitination of Chs3.

localization did not change after carbon source exchange (Supplemental Figure S4C), arguing against any direct control of Chs3 traffic by Snf1-mediated phosphorylation of Art4/Rod1 (Becuwe et al., 2012). It is therefore possible that Art4/Rod1 simply recognizes Chs3 after its insertion in the PM in a functional context similar to the one described for Art1 as part of a PM quality control system (Zhao et al., 2013). Moreover, Chs3 remained partially ubiquitinated in the absence of Art4/Rod1, a clear indication for additional sources of Chs3 ubiquitination. Of interest, the Chs3[1K] protein, which lacked the 1157 C-terminal lysine, conferred moderate resistance to calcofluor without affecting its LE endosomal traffic, a result that suggests reduced early turnover of this protein along the endosomal pathway and points to additional roles of ubiquitination on Chs3 traffic.

Our results thus indicate that the intracellular traffic of Chs3 is even more complex than anticipated and that several mechanisms cooperate in regulating its intracellular traffic in order to maintain the intracellular reservoir of Chs3 at the TGN/EE compartment (see Figure 7 for a model of Chs3 traffic). None of these mechanisms is new, but what is new, to our knowledge, is the convergence of all of these mechanisms in the regulation of the traffic of a single protein, Chs3, which reinforces its role as a model in the study of intracellular trafficking of proteins.

MATERIALS AND METHODS
Yeast strains and growth conditions
Most of the strains used in this work (see Supplemental Table S1) are derivatives of the single-gene-deletion mutant libraries from the European *Saccharomyces Cerevisiae* Archive for Functional Analysis (EUROSCARF, Bad Homburg, Germany) constructed in the BY4741/2 background, except for the *rsp5-1* strain, which belongs to the C. Boone thermosensitive collection (Li et al., 2011). When necessary, additional gene deletions were made using the gene replacement technique with different deletion cassettes based on

natMX4 or hphMX4 resistance (Goldstein and McCusker, 1999). Proteins were tagged chromosomally at their C-terminus with 3xHA or 1xGFP using integrative cassettes amplified from pFA6a-3HA-hphMx6 or pFA6a-GFP-hphMx6, respectively (Sato et al., 2005). Characterization of Chs3 function or localization was always made in a *chs3Δ::natMX4* strain containing a unique copy of the desired *CHS3* expressed from a centromeric plasmid under control of its own promoter. These strains also contained the pRS423::*CHS7* plasmid to diminish Chs3 retention at the ER. In addition, Chs3 was tagged at its endosomal locus with a 2xGFP tag placed at its C-terminus as previously described (Rockenbauch et al., 2012).

General methods for yeast handling have been previously described (Rose et al., 1990). Briefly, yeasts were transformed by the standard lithium acetate/polyethylene glycol procedure. Yeast cells were grown in 1% Bacto yeast extract/2% peptone/2% glucose or SD medium (2% glucose, 0.7% Difco yeast nitrogen base without amino acids) supplemented with the relevant amino acids at 28°C, except for the *rsp5-1* mutant, which was grown at the permissive temperature of 25°C. Stress experiments where performed by shifting cells from 25 to 39°C. For glycerol induction, cells were grown overnight in SD-Glc, harvested in the early exponential phase, resuspended in the same volume of SD-glycerol, and grown for 3 h. Calcofluor white resistance was tested by a plate assay on SD medium buffered with 50 mM potassium hydrogen phthalate, pH 6.2, as previously described (Trilla et al., 1999). When required, endocytosis was blocked using the actin-depolymerizing drug LatA (Enzo Life Science, Farmingdale, NY) at a final concentration of 0.03 mM (Reyes et al., 2007) for at least 20 min.

Plasmid construction
The Chs3[K1157R] (Chs3[1K]) and Chs3[K118/119/123/136R] (Chs3[4K]) mutants were generated by site-direct mutagenesis, as described, using the plasmid pRS315::*CHS3-GFP* (Trilla et al., 1999) as a template.

The Chs3[K118/119/123/136/1157R] (Chs3[5K]) mutant was remade from the Chs3[1K] and Chs3[4K] construct using *SalI/Hin*dIII restriction sites. Finally, the Chs3[K118/119/123/136/1125/1126/1157R] (Chs3[7K]) mutant was generated again by site-direct mutagenesis, using this time the pRS315::*Chs3[5K]-GFP* plasmid as a template. To obtain the Chs3[K118/119/123/136/492/511/586/592/612/702/723/1125/1126/1157R] (Chs3[14K]) mutant, a synthetic fragment of Chs3 carrying the K492/511/586/592/612/702/723R mutations was generated (Invitrogen) and transformed into *Saccharomyces cerevisiae* together with plasmid pRS315::*Chs3[7K]-GFP* linearized with *Pac*I. The plasmid generated by homologous recombination was recovered in *Escherichia coli* and sequenced to confirm the presence of the expected Chs3[14K]-GFP construct.

The introduction of a ubiquitin tag in the N-terminal extreme of Chs3 was done as follows. First, we created a pRS314::*CHS3* plasmid containing a single *Nco*I site at the first codon of *CHS3*. This plasmid was linearized with *Nco*I and cotransformed into yeast with a single ubiquitin cassette amplified by PCR from the *UBI4* gene using forward (Chs3-UbiF:GTCCCATTTTCTTCAAAGGTCCTGTTTAGACTATCCGCA GGAAAGatgcagatttttcgtcaagac) and reverse (Chs3-UbiR:TTAAGGTTCAGATAGT AGTCATCAGGATCATCTCCATTCAAGCC-GGTCATaccacctcttagccttagca) hybrid primers containing the appropriate flanking regions of *CHS3* to direct homologous recombination. Recombinant plasmids were rescued and sequenced to confirm the construct. The pRS315::[Ub]Chs3-GFP was obtained afterward by conventional subcloning using the *SacI/Hin*dIII restriction sites.

The N- and C-terminal truncations of Chs3 with their corresponding tags have been previously described (Sacristan *et al.*, 2013). The L24A mutation (Starr *et al.*, 2012) was created by site-directed mutagenesis on the corresponding plasmids. To generate the pRS315::*Chs3-HBH* plasmid, we amplified the HBH cassette (Tagwerker *et al.*, 2006) from the strain YPH499 Chs3::HBH by PCR, a strain kindly supplied by A. Spang (University of Basel). The cassette was then cloned at the C-terminal end of pRS315::*Chs3* using the *Hin*dIII/*Sph*I restriction sites. To address the degree of ubiquitination of Chs3, the YEplac195 plasmid was used for expression of 7xHis- tagged ubiquitin under control of the *CUP1* promoter. The empty plasmids served as controls (Parker *et al.*, 2007).

All constructs were confirmed by sequencing. See Supplemental Table S2 for a complete and detailed list of the plasmids used throughout this work.

Fluorescence microscopy
Chitin staining was observed in cells grown in the presence of 50 µg/ml calcofluor for 1 h at 28°C. Yeast cells expressing GFP-tagged proteins were grown to early logarithmic phase in SD medium supplemented with 0.2% adenine. In both cases, living cells were visualized directly by fluorescence microscopy. To stain vacuolar membranes, the lipophilic dye FM4-64 was added at 10 µM concentration to a culture of logarithmically growing cells. Thirty minutes after the addition of the dye, cells were washed twice with SD medium and observed using a fluorescence microscope.

Imaging was carried out using a Nikon 90i epifluorescence microscope (100× objective; numerical aperture 1.45) equipped with a Hamamatsu ORCA ER digital camera. Images were obtained by using the 49000 ET–4′,6-diamidino-2-phenylindole, 49002 ET-GFP (FITC/Cy2), and 49005 ET-DsRed (tetramethylrhodamine isothiocyanate/Cy3) filters (Chroma Technology). The images were then processed using ImageJ software (National Institutes of Health, Bethesda, MD) and Photoshop CS5 (Adobe, San José, CA) software. Line scans were also performed using the ImageJ software. All images shown in each series were acquired under identical condi-

tions and processed in parallel to preserve the relative intensities of fluorescence for comparative purposes. In all figures, the white scale bar represents 5 µM. When necessary, image measurements were statistically evaluated using analysis of variance and Student's *t* test for unpaired data and analyzed using GraphPad Prism software (GraphPad Software, La Jolla, CA). Significantly different values are indicated (*$i < 0.05$, **$p < 0.01$, ***$p < 0.001$, ****$p < 0.0001$).

Protein extracts and immunoblotting
Total cell lysates were prepared by resuspending cells obtained from 30 ml of logarithmic cultures in 150 µl of lysis buffer (50 mM Tris-HCl, pH 8, 0.1% Triton, 150 mM NaCl) containing 1× protease inhibition cocktail (1 mM phenylmethylsulfonyl fluoride [PMSF], 1 µg/ml aprotinin, 1 µg/ml leupeptin). Cells were disrupted using glass beads (0.45 mm; Sigma-Aldrich, St. Louis, MO) and three pulses of 30 s at the intensity of 5.5 U in a FastPrep (FP120 BIO101; MP Biomedicals, Santa Ana, CA). Cell debris was eliminated by centrifugation (5 min, $10,000 \times g$, 4°C), and the resultant supernatant was boiled for 5 min with 4× SDS loading buffer. Typically, 100 µg of protein per sample was separated using 7.5% SDS–PAGE gels and transferred onto polyvinylidene fluoride membranes (Trilla *et al.*, 1999). After being blocked with skimmed milk, the membranes were incubated with the corresponding antibodies: anti-GFP JL-8 monoclonal antibody (Living Colors; Takara Bio, Shiga, Japan), anti-HA 12CA5 (Roche, Basel Switzerland), anti-tubulin (T5162; Sigma-Aldrich, anti-6xHIS (H-15; Santa Cruz Biotechnology, Santa Cruz, CA), or anti–N-terminal fragment of Chs3 (Trautwein *et al.*, 2006). Blots were developed using the ECL kit (Advansta, Menlo Park, CA).

Tandem affinity purification of HBH-tagged proteins
The Chs3 protein tagged with the HBH cassette was purified as previously described (Tagwerker *et al.*, 2006). This double tag allowed for a first purification with nickel-nitriloacetic acid His-Bind resin (Novagen, Royston, UK) and a second one with Streptavidin Agarose Resin (Thermo Fisher Scientific, Waltham, MA). Purification was performed in denaturing conditions using 8 M urea. All buffers also contained 1× protease inhibition cocktail (1 mM PMSF, 1 µg/ml aprotinin, 1 µg/ml leupeptin) and 20 mM *N*-ethylmaleimide (NEM).

Pull down of His-tagged proteins
The degree of ubiquitination of Chs3 in different conditions was determined by pull-down assay as follows. Cells containing the Chs3-3xHA and the 7xHis-tagged ubiquitin plasmid growing logarithmically were induced with 0.1 mM CuSO4 for 45 min. Cells from 50-ml cultures were collected by centrifugation ($3200 \times g$, 4 min), washed once with cold water, resuspended in 500 µl of 12% trichloroacetic acid to denature the proteins, washed in 500 µl of 1 M Tris, pH 8, to restore pH, and collected by centrifugation. Cells were lysed with glass beads in 250 µl of buffer A (8 M urea, 7 mM NaH$_2$PO$_4$, 94 mM Na$_2$HPO$_4$, 10 mM Tris-HCl, pH 7.5, 0.05% Tween-20) containing a 1× protease inhibition cocktail as described earlier. Cell debris was removed by adding 500 µl of buffer A and then centrifuging the samples for 10 min at $15,000 \times g$. After measurement of the protein concentration, 100 µg of protein was saved as sample input. Supernatant corresponding to 0.5 mg of protein was brought up to 1 ml with buffer A and mixed with 70 µl of TALON metal affinity resin (Takara) previously equilibrated with buffer A and 15 mM imidazole to reduce unspecific binding to the beads. Mixtures were incubated at room temperature in an orbital rotator for 2 h. Subsequently the samples were washed three times with buffer A and three times with buffer C (8 M urea, 88 mM NaH$_2$PO$_4$, 12 mM Na$_2$HPO$_4$, 10 mM Tris-HCl, pH 7.5, 0.05% Tween-20). Proteins were then eluted with

40 µl of 2xSSR (4% SDS, 0.25 M Tris-HCl, pH 6.8, 10% sucrose, 0.025% bromophenol blue, 1% β-mercaptoethanol) for 3 min at 95°C and then loaded onto a SDS–PAGE gel. The Chs3-3xHA protein was visualized by immunoblotting, as explained earlier. All buffers also contained 20 mM NEM. Only the ubiquitinated forms of Chs3-3xHA should be visible after TALON binding, but the occasional appearance of faint bands in the untagged negative controls was noted, probably due to the unspecific binding of Chs3-3xHA to the resin. In all experiments, pull-down lanes contained five times the amount of protein loaded in the input lanes.

Coimmunoprecipitation

Yeast cells from a 200-ml logarithmically growing culture were harvested ($3200 \times g$, 4 min) and washed with cold water. Then cells were washed with 5 ml of stop buffer (154 mM NaCl, 10 mM ethylene diamine tetraacetic acid [EDTA], 10 mM NaN$_3$, 10 mM NaF) and 1.5 ml of wash buffer (50 mM Tris, pH 7.5, 5 mM EDTA). Cells were resuspended in 800 µl of lysis buffer (50 mM Tris, pH 7.5, 200 mM NaCl, 5 mM EDTA, 0.1% Triton) with 2× protease inhibition cocktail and broken with glass beads, and the lysate was clarified as described. Samples were diluted with lysis buffer to a final protein concentration of 2 mg/ml. Subsequently 1 ml of the protein sample was incubated with 50 µl of anti-HA or anti-GFP MicroBeads (Miltenyibiotec, Bergisch Gladbach, Germany) and 2% bovine serum albumin for 30 min at 4°C in an orbital rotator. Then mixtures were applied onto µColumns, placed into the µMACS Separator, and washed with the different kit buffers following the instructions provided by the manufacturer. Proteins specifically bound to the anti-HA or anti-GFP MicroBeads were eluted with 50 µl of elution buffer, preheated to 95°C, and applied directly to the column. Finally, all samples were boiled for 5 min and then separated in a 7.5% SDS–PAGE gel. Proteins were visualized by immunoblotting.

In the cases in which a cross-linking reaction was required, protein extracts adjusted to 2 mg/ml were incubated with 0.1 mM DSP cross-linker (Thermo Fisher Scientific) dissolved in dimethyl sulfoxide for 30 min at 22°C. Samples were then treated with 100 mM Tris-HCl, pH 7.4, for 15 min at 22°C to neutralize free reactive groups. These samples were incubated with MicroBeads and processed as previously described.

The levels of coIP were determined by measuring bands intensity with Quantity One software (Bio-Rad, Hercules, CA), and the relationship between the amounts of the pull-down and the coimmunoprecipitated proteins was established. The quantitative results presented are the average of several independent experiments.

REFERENCES

Alvaro CG, O'Donnell AF, Prosser DC, Augustine AA, Goldman A, Brodsky JL, Cyert MS, Wendland B, Thorner J (2014). Specific α-arrestins negatively regulate Saccharomyces cerevisiae pheromone response by down-modulating the G-protein-coupled receptor Ste2. Mol Cell Biol 34, 2660–2681.

Barfield RM, Fromme JC, Schekman R (2009). The exomer coat complex transports Fus1p to the plasma membrane via a novel plasma membrane sorting signal in yeast. Mol Biol Cell 20, 4985–4996.

Becuwe M, Léon S (2014). Integrated control of transporter endocytosis and recycling by the arrestin-related protein Rod1 and the ubiquitin ligase Rsp5. Elife 3, e03307.

Becuwe M, Vieira N, Lara D, Gomes-Rezende J, Soares-Cunha C, Casal M, Haguenauer-Tsapis R, Vincent O, Paiva S, Léon S (2012). A molecular switch on an arrestin-like protein relays glucose signaling to transporter endocytosis. J Cell Biol 196, 247–259.

Belgareh-Touzé N, Léon S, Erpapazoglou Z, Stawiecka-Mirota M, Urban-Grimal D, Haguenauer-Tsapis R (2008). Versatile role of the yeast ubiquitin ligase Rsp5p in intracellular trafficking. Biochem Soc Trans 36, 791–796.

Bonifacino JS (2014). Adaptor proteins involved in polarized sorting. J Cell Biol 204, 7–17.

Cabib E, Arroyo J (2013). How carbohydrates sculpt cells: chemical control of morphogenesis in the yeast cell wall. Nat Rev Microbiol 11, 648–655.

Chapa-y-Lazo B, Allwood EG, Smaczynska-de Rooij II, Snape ML, Ayscough KR (2014). Yeast endocytic adaptor AP-2 binds the stress sensor Mid2 and functions in polarized cell responses. Traffic 15, 546–557.

Chen SH, Shah AH, Segev N (2011). Ypt31/32 GTPases and their F-Box effector Rcy1 regulate ubiquitination of recycling proteins. Cell Logist 1, 21–31.

Copic A, Starr TL, Schekman R (2007). Ent3p and Ent5p exhibit cargo-specific functions in trafficking proteins between the trans-Golgi network and the endosomes in yeast. Mol Biol Cell 18, 1803–1815.

Crapeau M, Merhi A, André B (2014). Stress conditions promote yeast Gap1 permease ubiquitylation and down-regulation via the arrestin-like Bul and Aly proteins. Biol Chem 289, 22103–22116.

Delley PA, Hall MN (1999). Cell wall stress depolarizes cell growth via hyper-activation of RHO1. J Cell Biol 147, 163–174.

Foote C, Nothwehr S (2006). The clathrin adaptor complex 1 directly binds to a sorting signal in Ste13p to reduce the rate of its trafficking to the late endosome of yeast. J Cell Biol 22, 615–626.

Goldstein AL, McCusker JH (1999). Three new dominant drug resistance cassettes for gene disruption in Saccharomyces cerevisiae. Yeast 15, 1541–1553.

Gomez A, Perez J, Reyes A, Duran A, Roncero C (2009). Slt2 and Rim101 contribute independently to the correct assembly of the chitin ring at the budding yeast neck in Saccharomycces cerevisiae. Eukaryot Cell 8, 1449–1559.

Henne WM, Buchkovich NJ, Emr SD (2011). The ESCRT pathway. Dev Cell 21, 77–91.

Hettema EH, Lewis MJ, Black MW, Pelham HR (2003). Retromer and the sorting nexins Snx4/41/42 mediate distinct retrieval pathways from yeast endosomes. EMBO J 22, 548–557.

Kota J, Ljungdahl PO (2005). Specialized membrane-localized chaperones prevent aggregation of polytopic proteins in the ER. J Cell Biol 168, 79–88.

Lauwers E, Erpapazoglou Z, Haguenauer-Tsapis R, André B (2010). The ubiquitin code of yeast permease trafficking. Trends Cell Biol 20, 196–204.

Levin DE (2011). Regulation of cell wall biogenesis in Saccharomyces cerevisiae: the cell wall integrity signaling pathway. Genetics 189, 1145–1175.

Li Z, Vizeacoumar FJ, Bahr S, Li J, Warringer J, Vizeacoumar FS, Min R, VanderSluis B, Bellay J, Devit M, et al. (2011). Systematic exploration of essential yeast gene function with temperature-sensitive mutants. Nat Biotechnol 29, 361–367.

Lilie SH, Brown SS (1994). Immunofluorescence localization of the unconventional myosin, Myo2p, and the putative kinesin-related protein, Smy1p, to the same regions of polarized growth in Saccharomyces cerevisiae. J Cell Biol 125, 825–842.

Lin CH, MacGurn JA, Chu T, Stefan CJ, Emr SD (2008). Arrestin-related ubiquitin-ligase adaptors regulate endocytosis and protein turnover at the cell surface. Cell 135, 714–725.

MacGurn JA, Hsu PC, Emr SD (2012). Ubiquitin and membrane protein turnover: from cradle to grave. Annu Rev Biochem 81, 231–259.

Nikko E, Pelham HR (2009). Arrestin-mediated endocytosis of yeast plasma membrane transporters. Traffic 10, 1856–1867.

Nothwehr SF, Ha SA, Bruinsma P (2000). Sorting of yeast membrane proteins into an endosome-to-Golgi pathway involves direct interaction of their cytosolic domains with Vps35p. J Cell Biol 16, 297–310.

O'Donnell AF, Apffel A, Gardner RG, Cyert MS (2010). Alpha-arrestins Aly1 and Aly2 regulate intracellular trafficking in response to nutrient signaling. Mol Biol Cell 21, 3552–3566.

O'Donnell AF, McCartney RR, Chandrashekarappa DG, Zhang BB, Thorner J, Schmidt MC (2015). 2-Deoxyglucose impairs Saccharomyces cerevisiae growth by stimulating Snf1-regulated and α-arrestin–mediated trafficking of hexose transporters 1 and 3. Mol Cell Biol 35, 939–955.

Parker JL, Bielen AB, Dikic I, Ulrich HD (2007). Contributions of ubiquitin- and PCNA-binding domains to the activity of Polymerase eta in Saccharomyces cerevisiae. Nucleic Acids Res 35, 881–889.

Piper RC, Cooper AA, Yang H, Stevens TH (1995). VPS27 controls vacuolar and endocytic traffic through a prevacuolar compartment in Saccharomyces cerevisiae. J Cell Biol 131, 603–617.

Raiborg C, Stenmark H (2009). The ESCRT machinery in endosomal sorting of ubiquitylated membrane proteins. Nature 458, 445–452.

Raymond CK, Howald-Stevenson I, Vater CA, Stevens TH (1992). Morphological classification of the yeast vacuolar protein sorting mutants: evidence for a prevacuolar compartment in class E vps mutants. Mol Biol Cell 3, 1389–1402.

Reyes A, Sanz M, Duran A, Roncero C (2007). Chitin synthase III requires Chs4p-dependent translocation of Chs3p into the plasma membrane. J Cell Sci 120, 1998–2009.

Ritz AM, Trautwein M, Grassinger F, Spang A (2014). The prion-like domain in the exomer-dependent cargo Pin2 serves as a trans-Golgi retention motif. Cell Rep 10, 249–260.

Robinson MS (2015). Forty years of clathrin-coated vesicles. Traffic 16, 1210–1238.

Rockenbauch U, Ritz AM, Sacristan C, Roncero C, Spang A (2012). The complex interactions of Chs5p, the ChAPs, and the cargo Chs3p. Mol Biol Cell 23, 4404–44015.

Roncero C (2002). The genetic complexity of chitin synthesis in fungi. Curr Genet 41, 367–378.

Rose MD, Wisnton F, Hieter P (1990). Methods in Yeast Genetics: A Laboratory Course Manual, Cold Spring Harbor, NY: Cold Spring Harbor Laboratory Press.

Rubio-Texeira M, Kaiser CA (2006). Amino acids regulate retrieval of the yeast general amino Acid permease from the vacuolar targeting pathway. Mol Biol Cell 17, 3031–3050.

Russell MR, Shideler T, Nickerson DP, West M, Odorizzi G (2012). Class E compartments form in response to ESCRT dysfunction in yeast due to hyperactivity of the Vps21 Rab GTPase. J Cell Sci 125, 5208–5220.

Sacristan C, Manzano-Lopez J, Reyes A, Spang A, Muniz M, Roncero C (2013). Dimerization of the chitin synthase Chs3 is monitored at the Golgi and affects its endocytic recycling. Mol Microbiol 90, 252–266.

Sacristan C, Reyes A, Roncero C (2012). Neck compartmentalization as the molecular basis for the different endocytic behaviour of Chs3 during budding or hyperpolarized growth in yeast cells. Mol Microbiol 83, 1124–1135.

Sanchatjate S, Schekman R (2006). Chs5/6 complex: a multiprotein complex that interacts with and conveys chitin synthase III from the trans-Golgi network to the cell surface. Mol Biol Cell 17, 4157–4166.

Santos B, Snyder M (1997). Targeting of chitin synthase 3 to polarized growth sites in yeast requires Chs5p and Myo2p. J Cell Biol 136, 95–110.

Sato M, Dhut S, Toda T (2005). New drug-resistant cassettes for gene disruption and epitope tagging in Schizosaccharomyces pombe. Yeast 22, 582–591.

Seaman MN (2012). The retromer complex—endosomal protein recycling and beyond. J Cell Sci 125, 4693–4702.

Seaman MN, Marcusson EG, Cereghino JL, Emr SD (1997). Endosome to Golgi retrieval of the vacuolar protein sorting receptor, Vps10p, requires the function of the VPS29, VPS30, and VPS35 gene products. J Cell Biol 137, 79–92.

Shi Y, Stefan CJ, Rue SM, Teis D, Emr SD (2011). Two novel WD40 domain-containing proteins, Ere1 and Ere2, function in the retromer-mediated endosomal recycling pathway. Mol Biol Cell 22, 4093–4107.

Spang A (2009). On the fate of early endosomes. Biol Chem 390, 753–759.

Starr TL, Pagant S, Wang CW, Schekman R (2012). Sorting signals that mediate traffic of chitin synthase III between the TGN/endosomes and to the plasma membrane in yeast. PLoS One 7, e46386.

Strochlic TI, Schmiedekamp BC, Lee J, Katzmann DJ, Burd CG (2008). Opposing activities of the Snx3-retromer complex and ESCRT proteins mediate regulated cargo sorting at a common endosome. Mol Biol Cell 19, 4694–4706.

Swaney DL, Beltrao P, Starita L, Guo A, Rush J, Fields S, Krogan NJ, Villén J (2013). Global analysis of phosphorylation and ubiquitylation cross-talk in protein degradation. Nat Methods 10, 676–682.

Tagwerker C, Flick K, Cui M, Guerrero C, Dou Y, Auer B, Baldi P, Huang L, Kaiser P (2006). A tandem affinity tag for two-step purification under fully denaturing conditions: application in ubiquitin profiling and protein complex identification combined with in vivo cross-linking. Mol Cell Proteomics 5, 737–748.

Trautwein M, Schindler C, Gauss R, Dengjel J, Hartmann E, Spang A (2006). Arf1p, Chs5p and the ChAPs are required for export of specialized cargo from the Golgi. EMBO J 25, 943–954.

Trilla JA, Duran A, Roncero C (1999). Chs7p, a new protein involved in the control of protein export from the endoplasmic reticulum that is specifically engaged in the regulation of chitin synthesis in *Saccharomyces cerevisiae*. J Cell Biol 145, 1153–1163.

Valdivia RH, Baggot D, Chuang JS, Schekman R (2002). The yeast Clathrin adaptor protein complex 1 is required for the efficeint retention of a subset of late Golgi membrane proteins. Dev Cell 2, 283–294.

Valdivia RH, Schekman R (2003). The yeasts Rho1p and Pkc1p regulate the transport of chitin synthase III. (Chs3p) from internal stores to the plasma membrane. Proc Natl Acad Sci USA 100, 10287–10292.

Weiskoff AM, Fromme JC (2014). Distinct N-terminal regions of the exomer secretory vesicle cargo Chs3 regulate its trafficking itinerary. Front Cell Dev Biol 2, 47.

Zanolari B, Rockenbauch U, Trautwein M, Clay L, Barral Y, Spang A (2011). Transport to the plasma membrane is regulated differently early and late in the cell cycle in *Saccharomyces cerevisiae*. J Cell Sci 124, 1055–1066.

Zhao Y, Macgurn JA, Liu M, Emr SD (2013). The ART-Rsp5 ubiquitin ligase network comprises a plasma membrane quality control system that protects yeast cells from proteotoxic stress. Elife 2, e00459.

Ziman M, Chuang JS, Schekman RW (1996). Chs1p and Chs3p, two proteins involved in chitin synthesis, populate a compartment of the *Saccharomyces cerevisiae* endocytic pathway. Mol Biol Cell 7, 1909–1919.